

# B-meson Dileptonic Decays in NMSSM with a Light CP-odd Higgs Boson

Zhaoxia Heng<sup>a</sup>, Robert J. Oakes<sup>b</sup>, Wenyu Wang<sup>c</sup>, Zhaohua Xiong<sup>d</sup>, Jin Min Yang<sup>c</sup>

<sup>a</sup> *Physics Department, Henan Normal University, Xinxiang 453007, China*

<sup>b</sup> *Department of Physics and Astronomy,  
Northwestern University, Evanston, IL 60208, USA*

<sup>c</sup> *Institute of Theoretical Physics, Academia Sinica, Beijing 100080, China*

<sup>d</sup> *Institute of Theoretical Physics, College of Applied Sciences,  
Beijing University of Technology, Beijing 100020, China*

## Abstract

In the next-to-minimal supersymmetric model (NMSSM) a light CP-odd Higgs boson is so far allowed by current experiments, which, together with a large  $\tan\beta$ , may greatly enhance the rare dileptonic decays  $B \rightarrow X_s \ell^+ \ell^-$  and  $B_s \rightarrow \ell^+ \ell^- \gamma$ . We examine these decays paying special attention to the new operator allowed by the light CP-odd Higgs boson. We find that in the parameter space allowed by current experiments like LEP II and  $b \rightarrow s \gamma$ , the branching ratios of these rare decays can be greatly enhanced and thus the existing experimental data on  $B \rightarrow X_s \mu^+ \mu^-$  can further stringently constrain the parameter space (especially the region with a super-light CP-odd Higgs boson and large  $\tan\beta$ ). In the surviving parameter space we give the predictions for other dileptonic decay branching ratios and also show the results for the forward-backward asymmetry.

PACS numbers: 14.80.Cp, 13.85.Qk, 12.60.Jv

## I. INTRODUCTION

Recently some non-minimal supersymmetric models such as the next-to-minimal supersymmetric model (NMSSM) have attracted much attention [1] since these models can solve the  $\mu$ -problem and alleviate the little hierarchy. In the NMSSM, for example, the  $\mu$ -term in the superpotential is forbidden by imposing a discrete  $Z_3$  symmetry and instead it is generated through the coupling between the two Higgs doublets and a newly introduced gauge singlet scalar which develops a vacuum expectation value of the order of the SUSY breaking scale. In this way, the  $\mu$  parameter at the weak scale can be naturally explained. The NMSSM can ameliorate the little hierarchy by either tuning the parameters to enhance the theoretical upper bound for the mass of the lightest CP-even Higgs boson or relaxing the LEP2 bound of 114 GeV through allowing for a light CP-odd Higgs boson ( $A_1$ ) with mass below  $2m_b$  [2].

It is interesting to note that in the NMSSM the lightness of such a CP-odd Higgs boson can be naturally predicted in the enlarged parameter space, and is also allowed by the LEP II data [1]. This light Higgs boson can not only alleviate the little hierarchy, but also can help to explain the observed anomaly in the decay  $\Sigma^+ \rightarrow p\mu^+\mu^-$  [3]. On the other hand, if a Higgs boson is indeed so light, its effects in some low energy processes may be sizable and thus are necessary to check [4, 5]. For a super light  $A_1$  the decay  $b \rightarrow A_1 s$  is open and an analysis has been performed in [4] (note that as analysed in [4], a small CP-odd Higgs mass is only protected from RGE-effects in the limit of large  $\tan\beta$ ). In this work we consider the full possible mass range of  $A_1$  (heavy, intermediately heavy and light) and check the NMSSM effects in the rare B meson dileptonic decays  $B \rightarrow X_s \ell^+ \ell^-$  and  $B_s \rightarrow \ell^+ \ell^- \gamma$  [6].

These rare dileptonic decays are induced by the flavor-changing neutral-current (FCNC)  $b \rightarrow s$  transition and are of special interest due to their relative cleanliness and high sensitivity to new physics. In the Standard Model (SM) such FCNC processes are suppressed and have very small branching ratios [7] but can be greatly enhanced in some new physics models [8, 9, 10, 11, 12, 13]. Since experimental data on  $B \rightarrow X_s \mu^+ \mu^-$  is available and the future LHCb or super B factory will further scrutinize B meson decays, these dileptonic decays serve as a good probe of new physics.

In supersymmetric models these dileptonic decays can be drastically enhanced by large  $\tan\beta$  since both the  $b \rightarrow s$  transition loops (such as the charged Higgsino loops) and the

Higgs couplings in the Higgs-propagated diagrams are proportional to  $\tan\beta$ . It has been shown (see e.g. [12]) that in the minimal supersymmetric model (MSSM) great enhancements are possible for these decays. In the context of NMSSM, in addition to the  $\tan\beta$  enhancement, the presence of a light CP-odd Higgs boson could further enhance these dileptonic decays. Thus, the parameter space, especially the region with a super light CP-odd Higgs boson and a very large  $\tan\beta$ , is constrained by the existing data on  $B \rightarrow X_s \mu^+ \mu^-$ . In our analysis we will examine the NMSSM effects in these dileptonic decays by scanning over the parameter space allowed by the LEP II experiments and the data on  $b \rightarrow s \gamma$ . We will show the  $2\sigma$  constraints from  $B \rightarrow X_s \mu^+ \mu^-$  on the parameter space and then give the predictions for other dileptonic decay branching ratios and forward-backward asymmetry.

A key point in our calculations is the presence of a new operator due to the light CP-odd Higgs boson. In contrast to the MSSM, where all Higgs bosons and sparticles are so heavy that they can be integrated out at the weak scale, the light CP-odd Higgs boson  $A_1$  in the NMSSM cannot be integrated out at the weak scale and thus a new operator  $\mathcal{O}_A$  describing the interaction  $A_1 b \bar{s}$  must be treated carefully.

This work is organized as follows. In Sec. II a brief description of the NMSSM is presented. In Sec. III we calculate the Wilson coefficients paying special attention to the new operator  $\mathcal{O}_A$ . In Sec. IV we evaluate the NMSSM effects on the dileptonic decay branching ratios and the forward-backward (FB) asymmetry, and present some numerical results. The conclusion is given in Sec. V and analytical expressions from our calculations are presented in the Appendix.

## II. A BRIEF DESCRIPTION OF NMSSM

In the NMSSM a singlet Higgs superfield  $\hat{S}$  is introduced. A discrete  $\mathbb{Z}_3$  symmetry is imposed and thus only the cubic and trilinear terms are allowed in the superpotential. The Higgs terms in the superpotential are then given by

$$\lambda \hat{S} \hat{H}_u \cdot \hat{H}_d + \frac{\kappa}{3} \hat{S}^3. \quad (1)$$

Note that there is no explicit  $\mu$ -term and an effective  $\mu$ -parameter is generated when the scalar component ( $S$ ) of  $\hat{S}$  develops a vacuum expectation value  $s/\sqrt{2}$ :

$$\mu_{eff} = \lambda \langle S \rangle = \frac{s\lambda}{\sqrt{2}}. \quad (2)$$

The corresponding soft SUSY-breaking terms are given by

$$A_\lambda \lambda S H_u \cdot H_d + \frac{A_\kappa}{3} \kappa S^3. \quad (3)$$

The scalar Higgs potential is then given by

$$V_F = |\lambda H_u \cdot H_d + \kappa S^2|^2 + |\lambda S|^2 (|H_d|^2 + |H_u|^2), \quad (4)$$

$$V_D = \frac{g_2^2}{2} (|H_d|^2 |H_u|^2 - |H_u \cdot H_d|^2) + \frac{G^2}{8} (|H_d|^2 - |H_u|^2)^2, \quad (5)$$

$$V_{\text{soft}} = m_d^2 |H_d|^2 + m_u^2 |H_u|^2 + m_s^2 |S|^2 + \left( A_\lambda \lambda S H_u \cdot H_d + \frac{\kappa}{3} A_\kappa S^3 + h.c. \right), \quad (6)$$

where  $G^2 = g_1^2 + g_2^2$  with  $g_1$  and  $g_2$  being the coupling constants of  $U_Y(1)$  and  $SU_L(2)$ , respectively.

The scalar fields are expanded as follows:

$$H_d = \begin{pmatrix} \frac{1}{\sqrt{2}}(v_d + \phi_d + i\varphi_d) \\ H_d^- \end{pmatrix}, H_u = \begin{pmatrix} H_u^+ \\ \frac{1}{\sqrt{2}}(v_u + \phi_u + i\varphi_u) \end{pmatrix}, S = \frac{1}{\sqrt{2}}(s + \sigma + i\xi). \quad (7)$$

The mass eigenstates can be obtained by unitary rotations

$$\begin{pmatrix} H_1 \\ H_2 \\ H_3 \end{pmatrix} = U^H \begin{pmatrix} \phi_d \\ \phi_u \\ \sigma \end{pmatrix}, \begin{pmatrix} A_1 \\ A_2 \\ G_0 \end{pmatrix} = U^A \begin{pmatrix} \varphi_d \\ \varphi_u \\ \xi \end{pmatrix}, \begin{pmatrix} G^+ \\ H^+ \end{pmatrix} = U \begin{pmatrix} H_d^+ \\ H_u^+ \end{pmatrix}, \quad (8)$$

where  $H_{1,2,3}$  and  $A_{1,2}$  are respectively the CP-even and CP-odd neutral Higgs bosons,  $G^0$  and  $G^+$  are Goldstone bosons, and  $H^+$  is the charged Higgs boson. It is clear that the charged Higgs sector is the same as in the MSSM, while the neutral Higgs sector contains one more CP-even and one more CP-odd Higgs boson.  $U^A$  and  $U^H$  are given by

$$U^A = \begin{pmatrix} C_{\theta_A} S_\beta & C_{\theta_A} C_\beta & S_{\theta_A} \\ -S_{\theta_A} S_\beta & -S_{\theta_A} C_\beta & C_{\theta_A} \\ -C_\beta & S_\beta & 0 \end{pmatrix}, U^H = \begin{pmatrix} \frac{1}{\tan\beta}(C_{\theta_H} - \frac{v}{s}\delta_+ S_{\theta_H}) & C_{\theta_H} & -S_{\theta_H} \\ \frac{1}{\tan\beta}(S_{\theta_H} + \frac{v}{s}\delta_+ C_{\theta_H}) & S_{\theta_H} & C_{\theta_H} \\ 1 & \frac{-1}{\tan\beta} & \frac{-v}{s \tan\beta} \delta_+ \end{pmatrix}, \quad (9)$$

where  $C_X = \cos X$  and  $S_X = \sin X$  ( $X = \theta_A, \theta_H$ ). The mixing angles are given by [14]

$$\theta_A = \frac{\pi}{2} + \frac{v}{s \tan\beta} \delta_- + \mathcal{O}\left(\frac{1}{\tan^2\beta}\right), \quad \tan(2\theta_H) = \frac{2\lambda^2 v s}{2\kappa^2 s^2 - m_Z^2} \quad (10)$$

with  $v \simeq 246$  GeV and

$$\delta_\mp = \frac{\sqrt{2} A_\lambda \mp 2\kappa s}{\sqrt{2} A_\lambda + \kappa s}. \quad (11)$$

The Lagrangian of the Higgs couplings to quarks for a large  $\tan\beta$  are given by

$$\mathcal{L}_{A_i\bar{d}d} = -i\frac{g_2 m_d}{2m_W} \left( \frac{v}{s}\delta_- A_1, \tan\beta A_2 \right) \bar{d}\gamma_5 d, \quad (12)$$

$$\mathcal{L}_{A_i\bar{u}u} = -i\frac{g_2 m_u}{2m_W} \frac{1}{\tan\beta} \left( \frac{\delta_- v}{s \tan\beta} A_1, A_2 \right) \bar{u}\gamma_5 u, \quad (13)$$

$$\mathcal{L}_{(H_1, H_2, H_3)\bar{d}d} = -\frac{g_2 m_d}{2m_W} \left( (C_\theta - \frac{v}{s}\delta_+ S_\theta)H_1, (S_\theta + \frac{v}{s}\delta_+ C_\theta)H_2, \tan\beta H_3 \right) \bar{d}d, \quad (14)$$

$$\mathcal{L}_{(H_1, H_2, H_3)\bar{u}u} = -\frac{g_2 m_u}{2m_W} \left( C_\theta H_1, S_\theta H_2, -\frac{H_3}{\tan\beta} \right) \bar{u}u. \quad (15)$$

Here one can see that the coupling of the neutral CP-odd Higgs  $A_i$  with up-type quarks are suppressed by a large  $\tan\beta$  and thus can be neglected in the large  $\tan\beta$  limit.

Since one more Higgs superfield  $\hat{S}$  is introduced in the NMSSM, we have a new neutral Higgsino  $\psi_S$ . So the neutralino sector is composed of  $U_Y(1)$  gaugino  $\lambda^1$ ,  $SU_L(2)$  gaugino  $\lambda^2$ , and the Higgsinos  $\psi_{H_d}^1$ ,  $\psi_{H_u}^2$  and  $\psi_S$ . The corresponding mass terms are given by

$$\begin{aligned} \mathcal{L}_{m_\chi^0} &= i\frac{1}{2}v(g_2\lambda^2 - g_1\lambda^1)(\cos\beta\psi_{H_d}^1 - \sin\beta\psi_{H_u}^2) - \frac{1}{2}M_2\lambda^2\lambda^2 - \frac{1}{2}M_1\lambda^1\lambda^1 - \frac{1}{\sqrt{2}}\lambda_S\psi_{H_d}^1\psi_{H_u}^2 \\ &\quad - \frac{1}{\sqrt{2}}v\lambda(\cos\beta\psi_{H_u}^2\psi_S + \sin\beta\psi_{H_d}^1\psi_S) + \frac{1}{\sqrt{2}}\kappa_S\psi_S^2 + \text{h.c.} \\ &= -\frac{1}{2}(\psi^0)^T Y_{\chi^0} \psi^0 + \text{h.c.}, \end{aligned} \quad (16)$$

where

$$(\psi^0)^T = (-i\lambda^1, -i\lambda^2, \psi_{H_d}^1, \psi_{H_u}^2, \psi_S). \quad (17)$$

The neutralinos are obtained by the unitary rotation  $\psi_i^0 = (Z_N)_{ij}\chi_j^0$ , where  $Z_N$  diagonalizes the mass matrix  $Y_{\chi^0}$ .

Similar to the charged Higgs sector, the chargino sector of the NMSSM is the same as in the MSSM with  $\mu$  replaced by  $\mu_{eff}$ . The chargino masses are obtained by the diagonalization of the mass matrix with two unitary matrices  $Z_-$  and  $Z_+$ :

$$M_{\chi^c} = (Z_-)^T \begin{pmatrix} -M_2 & \sqrt{2}m_W \sin\beta \\ \sqrt{2}m_W \cos\beta & -\mu_{eff} \end{pmatrix} Z_+. \quad (18)$$

### III. CALCULATIONS OF WILSON COEFFICIENTS

In our calculations we consider the flavor mixing between  $\tilde{b}$  and  $\tilde{s}$ , which make contributions to the dileptonic B meson decays through gluino or neutralino loops. Following the

analysis in [15], we assume the flavors are diagonal at tree level and the mixings are induced at loop level. Such mixings can be parameterized by a small mixing parameter  $\epsilon_1$  which is dependent on some soft-breaking mass parameters [15]. In our numerical calculations we input  $\epsilon_1 = 0.1$  for illustration. We perform the calculations in the Feynman gauge and thus the Goldstone bosons will be involved in the loop diagrams.

Since in the NMSSM the lighter mass eigenstate, the CP-odd neutral Higgs boson  $A_1$ , can be rather light, with a mass ranging from 100 MeV to the weak scale [1, 2] ( using the package NMHDECAY [16], we checked that such a light CP-odd Higgs boson  $A_1$  is indeed allowed by the LEP II data), in our calculations we pay special attention to this wide mass range of  $A_1$  and discriminate three cases.

(i) *Case A: Heavy  $A_1$ .*

For a heavy  $A_1$ , around weak scale, we integrate it out together with the other heavy particles (Higgs bosons, top quark,  $W^\pm$  and  $Z$  bosons, sparticles) at weak scale to obtain the Wilson coefficients. The effective Hamiltonian describing  $b \rightarrow sl^+l^-$  transition reads

$$\mathcal{H}_{eff} = -\frac{4G_F}{\sqrt{2}}V_{tb}V_{ts}^* \left[ \sum_{i=1}^{10} C_i(\mu_r)\mathcal{O}_i(\mu_r) + \sum_{i=1}^2 C_{Q_i}(\mu_r)\mathcal{Q}_i(\mu_r) \right], \quad (19)$$

where  $\mathcal{O}_i$  and  $\mathcal{Q}_i$  are operators listed in [8, 12], and  $C_i$  and  $C_{Q_i}$  are respectively their Wilson coefficients, and  $\mu_r$  is the renormalization scale. Note that the most general Hamiltonian in low-energy supersymmetry also contains the operators  $\mathcal{O}'_i$  and  $\mathcal{Q}'_i$  which respectively are the flipped chirality partners of  $\mathcal{O}_i$  and  $\mathcal{Q}_i$ . However, they give negligible contributions and thus are not considered in the final discussion of physical quantities [17].

In this case, there are no new operators and we only need to calculate the NMSSM contributions to these coefficients  $C_i$  and  $C_{Q_i}$  at the scale of  $m_W$ . For the processes in our analysis, only  $C_{7,9,10}$  and  $C_{Q_{1,2}}$  are relevant. The NMSSM contributions to  $C_{7,9,10}$  are the same as in the MSSM, which are computed in [18]. For  $C_{Q_{1,2}}$  the NMSSM contributions are different from the MSSM contributions [12] and thus need to be calculated here. The Feynman diagrams we need to calculate are shown in Fig.1, where the loops respectively involve the charged Higgs bosons, charginos, gluinos and

neutralinos. From the calculations of these diagrams we obtain the Wilson coefficients at  $m_W$  scale, which are presented in the Appendix.

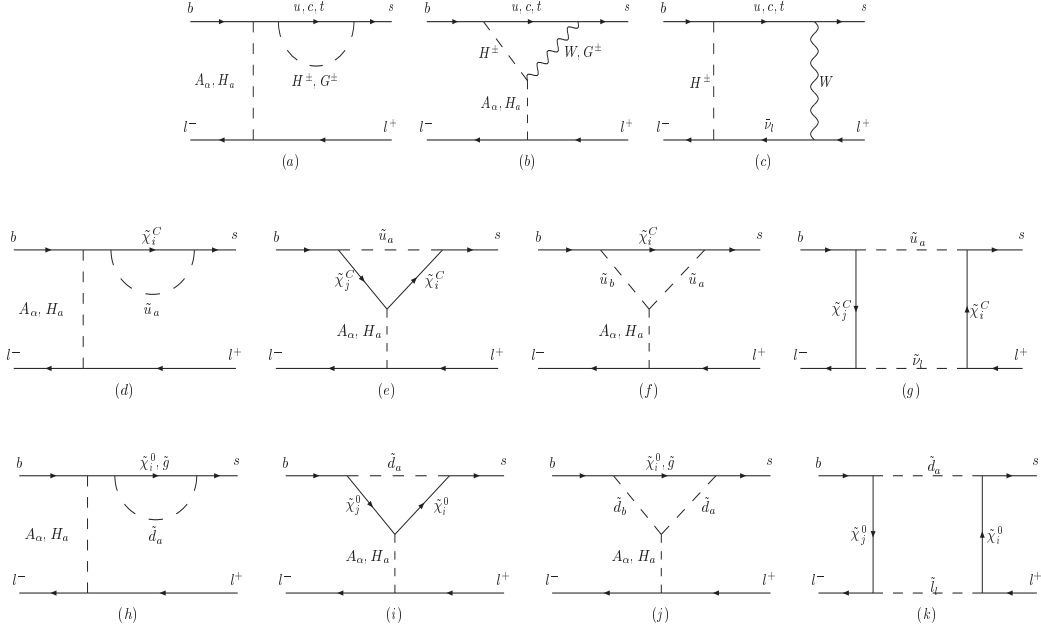


FIG. 1: The Feynman diagrams which give the dominate contributions to  $C_{Q_{1,2}}$ : (a-c) charged Higgs loops, (d-g) chargino loops, (h-k) gluino and neutralino loops.

For the calculation of the dileptonic B meson decays we need to know the Wilson coefficients at the  $m_b$  scale, which can be obtained from the running of the coefficients at the  $m_W$  scale down to the  $m_b$  scale. Such a running is governed by the anomalous dimension which can be found in [12].

(ii) *Case B*:  $A_1$  with an intermediate mass  $m_b \ll m_{A_1} \ll m_W$ .

At the  $m_W$  scale we retain  $A_1$  as an active field and thus we have a new operator  $\mathcal{O}_A$ . After integrating out all heavy particles at the  $m_W$  scale we obtain the Wilson coefficients including  $C_A$  for  $\mathcal{O}_A$ . Then we work out the anomalous dimensions and run the Wilson coefficients from the  $m_W$  scale to the  $m_{A_1}$  scale. At the  $m_{A_1}$  scale we integrate out  $A_1$ , which makes an additional contribution to  $C_{Q_i}(m_{A_1})$ . Finally, we run all the Wilson coefficients from the  $m_{A_1}$  scale to the  $m_b$  scale.

The new operator  $\mathcal{O}_A$  at the  $m_W$  scale takes the form

$$\mathcal{O}_A = i \frac{g_2}{16\pi^2} m_b m_W \bar{s}_L^\alpha b_R^\alpha A_1. \quad (20)$$

From the calculations of the corresponding diagrams in Fig. 1 we obtain the Wilson coefficient  $C_A(m_W)$ . It is composed of the charged Higgs loop contribution, the chargino loop contribution, the neutralino loop contribution and the gluino loop contribution, whose analytic expressions are given in the Appendix.

For the running of the Wilson coefficients including  $C_A$  from the  $m_W$  scale to the  $m_{A_1}$  scale we work out the anomalous dimensions by calculating one-loop diagrams with operator insertions. We find that all the Wilson coefficients in Eq.(19) run in the same way as in the MSSM [12], while the new coefficient  $C_A$  is not changed, i.e.,  $C_A(m_{A_1}) = C_A(m_W)$ .

When integrating out  $A_1$  at the  $m_{A_1}$  scale we find it gives a contribution  $\Delta C_{Q_2}(m_{A_1})$  to the operator  $\mathcal{Q}_2$

$$\Delta C_{Q_2}(m_{A_1}) = -\frac{\delta_- v m_b m_l}{2 s m_{A_1}^2} C_A(m_{A_1}). \quad (21)$$

Finally, for the running of the Wilson coefficients from the  $m_{A_1}$  scale to the  $m_b$  scale the anomalous dimensions are the same as in the MSSM [12].

(iii) *Case C*: Super light  $A_1$  with mass  $m_{A_1} < m_b$ .

In this case we retain  $A_1$  as an active field in the entire analysis. At the  $m_W$  scale we integrate out all heavy particles and obtain the Wilson coefficients including  $C_A$ . Then we run the coefficients down to the  $m_b$  scale. At the  $m_b$  scale the effects of  $\mathcal{O}_A$  are represented by a change in  $C_{Q_2}$

$$\Delta C_{Q_2}(m_b) = \frac{\delta_- v}{2 s} \frac{m_b m_l}{p^2 - m_{A_1}^2 + i m_{A_1} \Gamma_{A_1}} C_A(m_b), \quad (22)$$

where  $p$  is the momentum transfer and  $\Gamma_{A_1}$  is the total width of  $A_1$ . Since  $A_1$  can be on-shell in this case, the effects of  $A_1$  can be sizable even if without  $\tan \beta$  enhancement.

Note that the chargino loop contributions to  $C_A$  were also calculated in [4] where the corresponding diagrams induced by the  $A_1$ -squark-squark vertex are neglected since the author considered the large  $\tan \beta$  limit. In our numerical calculations we used the full results by keeping all terms and thus we also included the diagrams induced by the  $A_1$ -squark-squark coupling although they contain no leading  $\tan \beta$  terms. Except for the case of a large  $\tan \beta$ , such diagrams induced by the  $A_1$ -squark-squark coupling should be included since the  $A_1$ -squark-squark coupling can arise from the F-term of the superpotential and not suppressed



by the singleness of  $A_1$ . We checked that in the large  $\tan\beta$  limit we can reproduce the analytical result given in [4] for the chargino-loop contributions.

#### IV. DILEPTONIC B-MESON DECAYS IN NMSSM

With the effective Hamiltonian and the running of the Wilson coefficients presented in the preceding section we calculate the inclusive decays  $B \rightarrow X_s \ell^+ \ell^-$  and their forward-backward (FB) asymmetry, as well as the exclusive decays  $B_s \rightarrow \ell^+ \ell^- \gamma$ . The formulas in terms of the Wilson coefficients can be found in [8, 12].

Note that our supersymmetric contributions to the Wilson coefficients are given at one-loop level (next-to-leading order), while the SM contributions are known at two-loop level (next-to-next-to-leading order)[7]. In our numerical calculations we consider the one-loop results for the NMSSM, while for the SM we also include the two-loop results.

For the inclusive decays  $B \rightarrow X_s \ell^+ \ell^-$  we exclude the resonances  $J/\Psi$  and  $\Psi'$  contributions by using the same cuts as in the experiments [19], i.e., the invariant dilepton mass in the ranges

$$(2m_l, 2.75 \text{ GeV}) \oplus (3.3 \text{ GeV}, 3.39 \text{ GeV}) \oplus (3.84 \text{ GeV}, m_b), \quad (23)$$

so that our results can be compared with the experimental measurements.

For exclusive decays  $B_s \rightarrow \ell^+ \ell^- \gamma$  we follow [10, 12] and consider the photon in  $B_s \rightarrow \ell^+ \ell^- \gamma$  as a hard photon by imposing a cut on the photon energy  $E_\gamma$ , which means that the radiated photon can be detected in the experiments. This cut requires  $E_\gamma \geq \delta m_{B_s}/2$  with  $\delta = 0.02$ . (Note that for a soft photon both processes  $B_s \rightarrow \ell^+ \ell^- \gamma$  and  $B_s \rightarrow \ell^+ \ell^-$  must be considered together and in this case the infrared singular terms in  $B_s \rightarrow \ell^+ \ell^- \gamma$  are cancelled by the  $O(\alpha_{em})$  virtual corrections in  $B_s \rightarrow \ell^+ \ell^-$  [10].)

In our numerical calculations we perform a scan over the NMSSM parameter space

$$\begin{aligned} 2 \leq \tan\beta \leq 30, \quad -500 \text{ GeV} \leq \mu_{eff} \leq 500 \text{ GeV}, \\ -1 \leq \lambda \leq 1, \quad -1 \leq \kappa \leq 1, \\ -50 \text{ GeV} \leq A_\lambda \leq 50 \text{ GeV}, \quad -10 \text{ GeV} \leq A_\kappa \leq 10 \text{ GeV} \end{aligned} \quad (24)$$

with fixed parameters for the sfermion and gaugino sector (500 GeV for all sfermions and the gluino, and 200 GeV and 100 GeV for  $SU(2)$  and  $U(1)$  gaugino masses  $M_2$  and  $M_1$ , respectively). In our scan we consider the following constraints:

- (1) The LEP2 constraints by using the package NMHDECAY [16].
- (2) The constraints from  $B \rightarrow X_s \gamma$  which stringently constrain the effective coefficient  $C_7^{eff}$ . For the experimental result we use the world average value [20]

$$Br(B \rightarrow X_s \gamma)|_{exp} = (3.55 \pm 0.24_{-0.10}^{+0.09} \pm 0.03) \times 10^{-4}. \quad (25)$$

- (3) The constraints from  $B_s \rightarrow \mu^+ \mu^-$ , which constrain the Wilson coefficient  $C_A$  of the light pseudoscalar operator [4, 12]. The experimental result is given by [21]

$$Br(B_s \rightarrow \mu^+ \mu^-) < 1.5 \times 10^{-7} \quad (90\% \text{ C.L.}). \quad (26)$$

Among the relevant dileptonic decays experiment data is only available for  $Br(B \rightarrow X_s \mu^+ \mu^-)$ , which is given by [21]

$$Br(B \rightarrow X_s \mu^+ \mu^-) = (4.3 \pm 1.2) \times 10^{-6}. \quad (27)$$

In displaying our numerical results we will show this bound and use it to constrain the parameter space. For other dileptonic decay branching ratios, with no experiment data available, we will compare the NMSSM predictions with the SM values given by

$$Br(B \rightarrow X_s \tau^+ \tau^-) = 4.43 \times 10^{-8}, \quad (28)$$

$$Br(B_s \rightarrow \gamma \mu^+ \mu^-) = 1.33 \times 10^{-8}, \quad (29)$$

$$Br(B_s \rightarrow \gamma \tau^+ \tau^-) = 1.35 \times 10^{-8}. \quad (30)$$

Note that the SM prediction for  $Br(B \rightarrow X_s \tau^+ \tau^-)$  was also given in [22]. But our result is different from theirs because it is very sensitive to the cuts around the resonances  $J/\psi$  and  $\psi'$ . While our cuts are chosen as in Eq.(23), we cannot find the corresponding cuts used in [22]. We can easily reproduce the result in [22] by varying the cuts.

In Fig.2 we show the scatter plots of the branching ratio for  $B \rightarrow X_s \mu^+ \mu^-$  versus  $\tan \beta$ . Here we present the results for the three cases: a super light  $A_1$  ( $m_{A_1} < 5 \text{ GeV}$ ), an intermediately heavy  $A_1$  ( $5 \text{ GeV} < m_{A_1} < 40 \text{ GeV}$ ) and a heavy  $A_1$  at  $m_W$  scale. In order to see how stringent the  $b \rightarrow s \gamma$  constraints are we display the scatter plots with and without the  $b \rightarrow s \gamma$  constraints. From this figure we make the following observations: (1) The branching ratio can be greatly enhanced by large  $\tan \beta$ . (2)  $b \rightarrow s \gamma$  constraints are quite stringent and can exclude a large part of the parameter space, typically with large  $\tan \beta$ . (3) In the

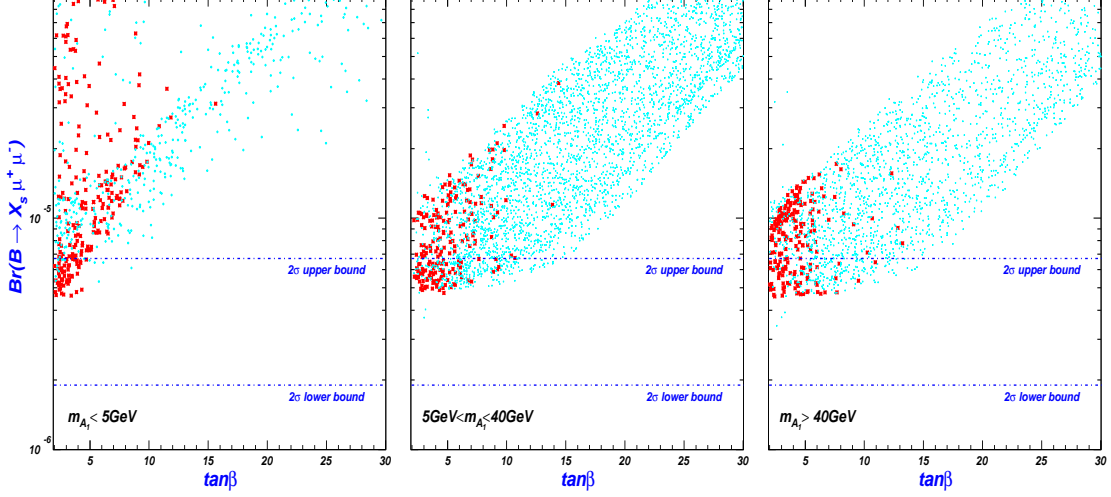


FIG. 2: Scatter plots for the branching ratio of  $B \rightarrow X_s \mu^+ \mu^-$  versus  $\tan \beta$ : the left panel is for a super light  $A_1$  ( $m_{A_1} < 5\text{GeV}$ ), the middle panel is for an intermediately heavy  $A_1$  ( $5\text{ GeV} < m_{A_1} < 40\text{ GeV}$ ) and the right panel is for a heavy  $A_1$  at  $m_W$  scale. The dark (red) points are allowed by  $b \rightarrow s\gamma$ , while the light (sky-blue) points are excluded by  $b \rightarrow s\gamma$ .

parameter space allowed by  $b \rightarrow s\gamma$  the decay  $B \rightarrow X_s \mu^+ \mu^-$  can still be greatly enhanced, especially in case of a super light  $A_1$ . The  $2\sigma$  experimental bound on  $B \rightarrow X_s \mu^+ \mu^-$  can further exclude a large part of the parameter space. Almost no points with  $\tan \beta > 15$  in the parameter space survive all the constraints. From the left panel of Fig.2 we see that some part of the parameter space with a super light  $A_1$  is still allowed by  $b \rightarrow s\gamma$  and  $B \rightarrow X_s \mu^+ \mu^-$ .

Let us take a look on the constraints from the process  $B_s \rightarrow \mu^+ \mu^-$ , whose branching ratio is given by [23]

$$\begin{aligned}
 Br(B_s \rightarrow \mu^+ \mu^-) &= 1.2 \times 10^{-7} \left[ \frac{\tau_{B_s}}{1.49 ps} \right] \left[ \frac{f_{B_s}}{245 MeV} \right]^2 \left| \frac{V_{ts}}{0.04} \right|^2 \left[ \frac{m_{B_s}}{5.37 GeV} \right]^3 \\
 &\times \left[ C_{Q_1}^2 + \left( C_{Q_2} + 2 \frac{m_\mu}{m_{B_s}} C_{10} \right)^2 \right]. \quad (31)
 \end{aligned}$$

We see that the contributions are from  $C_{10}$  and  $C_{Q_{1,2}}$ . While the contribution from  $C_{10}$  is suppressed by the factor  $m_\mu/m_{B_s}$ , the contributions from  $C_{Q_{1,2}}$  can be enhanced by large  $\tan \beta$  ( $C_{Q_{1,2}}$  contain terms which are proportional to  $\tan^3 \beta$ , as shown in the Appendix). This feature can be seen from Fig.3 in which we set aside the  $b \rightarrow s\gamma$  constraints and illustrated the  $B_s \rightarrow \mu^+ \mu^-$  constraints. We see that, similar to the  $b \rightarrow s\gamma$  constraints, the  $B_s \rightarrow \mu^+ \mu^-$  constraints are stringent for a large  $\tan \beta$ . If we impose the  $b \rightarrow s\gamma$  constraints

which exclude a very large  $\tan\beta$ , then the further constraints from  $B_s \rightarrow \mu^+\mu^-$  are stringent only for the parameter space with a very light  $A_1$ .

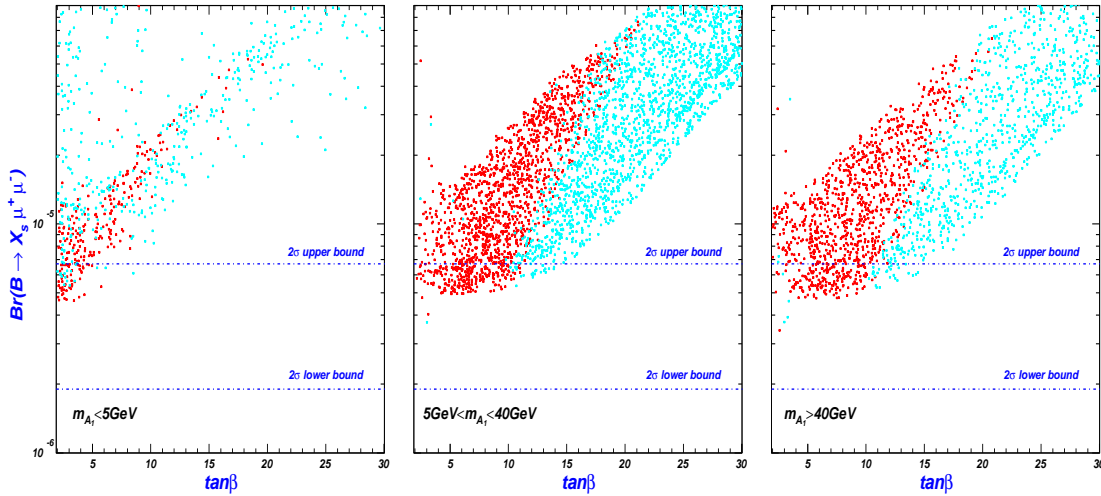


FIG. 3: Same as Fig.2, but with the  $B_s \rightarrow \mu^+\mu^-$  constraints. The dark (red) points are allowed by  $B_s \rightarrow \mu^+\mu^-$ , while the light (sky-blue) points are excluded by  $B_s \rightarrow \mu^+\mu^-$ .

The results for other dileptonic decay branching ratios, for which no experiment data are available, are presented in Fig.4. To see how stringent the constraints from  $B \rightarrow X_s \mu^+\mu^-$  are we display the scatter plots with and without such constraints (all the points satisfy  $b \rightarrow s\gamma$  and  $B_s \rightarrow \mu^+\mu^-$ ).

From Fig.4 we see that under the constraint from  $B \rightarrow X_s \mu^+\mu^-$ , the branching ratio of  $B \rightarrow X_s \tau^+\tau^-$  does not deviate significantly from the SM value. The reason is that these two decays are highly correlated except for the contributions of  $C_{Q_{1,2}}$  and  $C_A$  which are dependent on the lepton mass. If the contributions of  $C_{Q_{1,2}}$  and  $C_A$  are dominant, then  $Br(B \rightarrow X_s \tau^+\tau^-)$  should not be severely constrained by  $B \rightarrow X_s \mu^+\mu^-$ . As discussed below Eq.(31), the contributions of  $C_{Q_{1,2}}$  and  $C_A$  are important only for very large  $\tan\beta$  which is not allowed by  $b \rightarrow s\gamma$ . As a result, the contributions of  $C_{Q_{1,2}}$  and  $C_A$  are not dominant and thus  $B \rightarrow X_s \tau^+\tau^-$  is highly correlated to  $B \rightarrow X_s \mu^+\mu^-$ .

Note that for  $B \rightarrow X_s \tau^+\tau^-$  it may be rather challenging to disentangle the NMSSM effects from the SM value in future experiments. One reason is that, as discussed above, the NMSSM effects are no longer so sizable under the constraint of  $B \rightarrow X_s \mu^+\mu^-$ . The other reason is that the SM prediction has its own uncertainty. If we consider the uncertainty of the input SM parameters, we can obtain the uncertainty (about 20% as found in [22]) of the

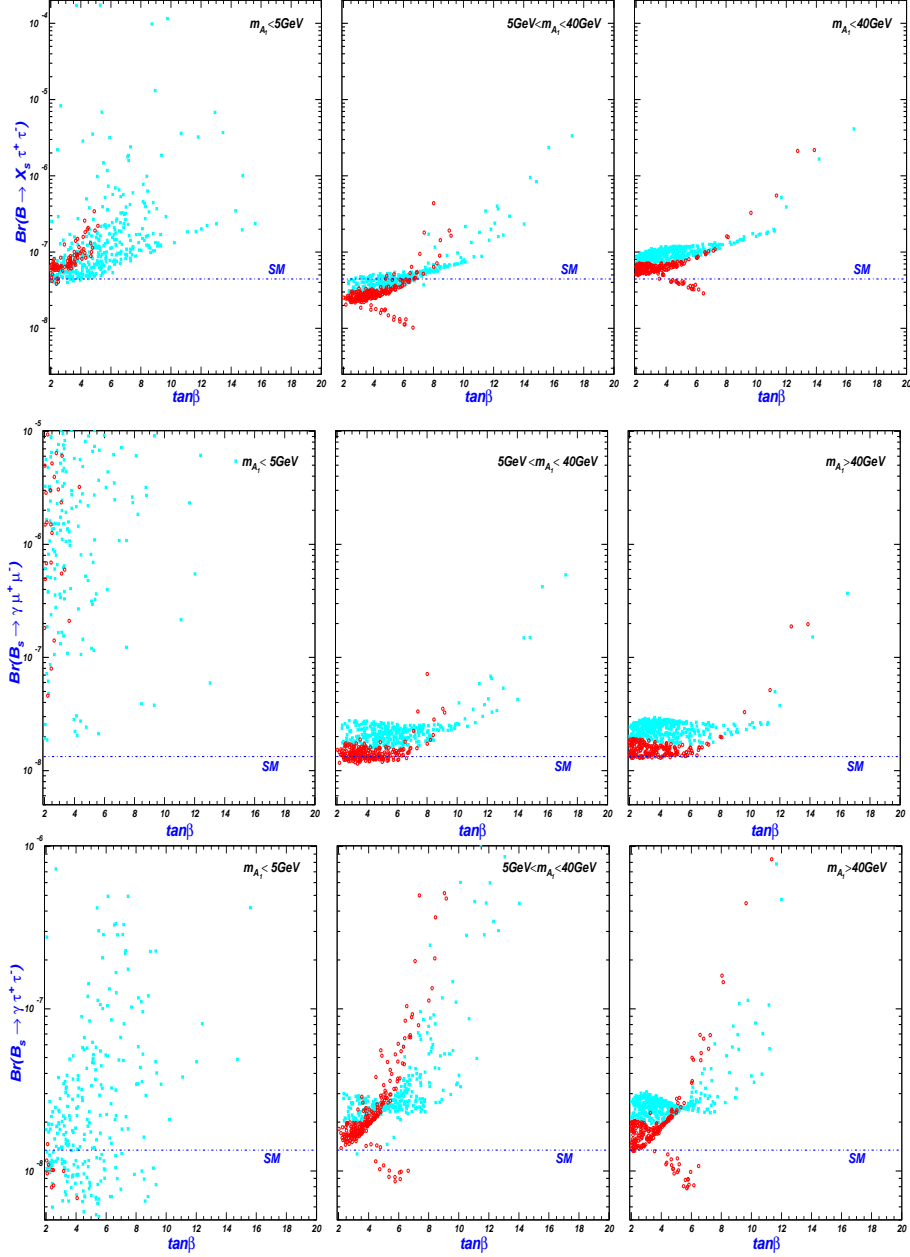


FIG. 4: Same as Fig.2, but for  $B \rightarrow X_s \tau^+ \tau^-$ ,  $B_s \rightarrow \gamma \mu^+ \mu^-$  and  $B_s \rightarrow \gamma \tau^+ \tau^-$ . The dark (red) points are allowed by  $B \rightarrow X_s \mu^+ \mu^-$ , while the light (sky-blue) points are excluded by  $B \rightarrow X_s \mu^+ \mu^-$ .

SM prediction. But in Fig.4 we did not show such an uncertainty of the SM value because for all the results, both NMSSM and SM, we used a same set of the SM parameters without allowing them to vary in the uncertainty range. Since the SM parameters are involved in both the NMSSM and SM values, all the results are subject to some uncertainty if we consider the uncertainty of the SM parameters. Of course, such uncertainties will deteriorate

the observability of the NMSSM effects.

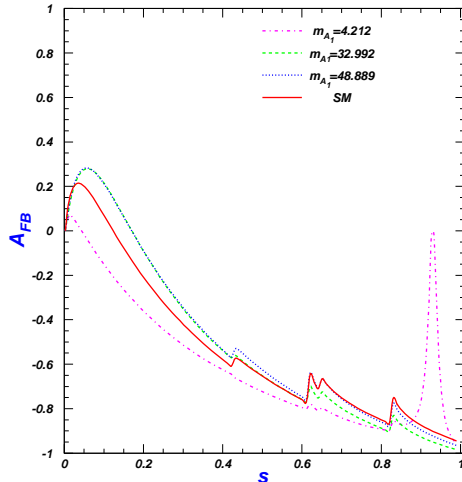


FIG. 5: The forward-backward asymmetry of  $B \rightarrow X_s \mu^+ \mu^-$  versus  $s = p^2/m_b^2$  ( $p^2$  is the invariant mass of  $\mu^+$  and  $\mu^-$ ).

Finally, in Fig.5 we show the results for the forward-backward asymmetry in  $B \rightarrow X_s \mu^+ \mu^-$  under the constraints from  $B \rightarrow X_s \mu^+ \mu^-$ .

## V. SUMMARY

In the framework of the NMSSM we examined the rare dileptonic decays  $B \rightarrow X_s \ell^+ \ell^-$  and  $B_s \rightarrow \ell^+ \ell^- \gamma$  paying particular attention to the light CP-odd Higgs boson. We found that in the parameter space allowed by current experiments, such as LEP II and  $b \rightarrow s \gamma$ , the branching ratios of these rare decays can be greatly enhanced and thus the experimental data on  $B \rightarrow X_s \mu^+ \mu^-$  further stringently constrains the parameter space, especially with a super light CP-odd Higgs boson and large  $\tan \beta$ . In the surviving parameter space we gave the NMSSM predictions for other unmeasured dileptonic decays which may hopefully be measured at the future LHCb or super B factory.

## Acknowledgment

We thank J. J. Cao, C. S. Huang, K. Hikasa and K. Tobe for discussions. This work was supported in part by National Natural Science Foundation of China (NNSFC) under grant No. 10725526 and 10635030, by the US Department of Energy, Division of High Energy

Physics under No. DE-FG02-91-ER4086 and by the JSPS invitation program under No. S-08034.

## APPENDIX A: WILSON COEFFICIENTS

The Wilson coefficients  $C_7$ ,  $C_9$  and  $C_{10}$  in the NMSSM are the same as in the MSSM [18]. Here we present the new coefficient  $C_A$ , and  $C_{Q_1}$  and  $C_{Q_2}$ , whose predictions in the NMSSM are different from the MSSM. We checked that we can analytically reproduce the MSSM results [12, 13, 18] (However, the NMSSM results can not explicitly reduce to the MSSM results by simply dropping out the singlet  $\hat{S}$  (say setting  $\lambda = \kappa = 0$ ) because the  $\mu$ -term is generated by  $\hat{S}$ ).

Although in our numerical calculations we used the complete results by keeping all terms, here, for simplicity, we only present the terms which can be enhanced by large  $\tan\beta$ . At the  $m_W$  scale each Wilson coefficient is composed of the charged Higgs loop contribution from Fig.1(a-c), the chargino loop contribution from Fig.1(d-g), the neutralino and gluino loop contribution from Fig.1(h-k).

For the charged Higgs contributions:

$$C_A^{H^\pm} = -\frac{i\lambda A_\lambda}{g_2 m_W} \tan\beta F_1(x_{H^\pm t}, x_{Wt}) \quad (\text{A1})$$

$$C_{Q_1}^{H^\pm} = -\frac{m_b m_l}{4m_{H_a}^2} \tan^2\beta \left[ \frac{m_{H^\pm}^2}{m_W^2} U_{a1}^H U_{a1}^H F_1(x_{H^\pm t}, x_{Wt}) + \frac{m_t^2 m_{H_a}^2}{m_W^2 m_{H^\pm}^2} F_1(x_{tH^\pm}, x_{tW}) \right] \quad (\text{A2})$$

$$C_{Q_2}^{H^\pm} = \frac{m_b m_l}{4m_{A_\alpha}^2} \tan^2\beta \left[ \left( \frac{m_{H^\pm}^2}{m_W^2} U_{\alpha 1}^A U_{\alpha 1}^A + \delta_{\alpha 2} U_{\alpha 1}^A \right) F_1(x_{H^\pm t}, x_{Wt}) + \frac{m_t^2 m_{A_\alpha}^2}{m_W^2 m_{H^\pm}^2} F_1(x_{tH^\pm}, x_{tW}) \right] \quad (\text{A3})$$

Note that although  $H^\pm W^\pm A_1$  vertex has  $1/\tan\beta$  suppression by the singleness of  $A_1$ ,  $H^\pm G^\pm A_1$  vertex which comes from the soft term  $A_\lambda \lambda S H_u^1 H_d^2$  does not have such  $1/\tan\beta$  suppression. Thus the contribution to  $C_A$  from the loop involving  $H^\pm$  and  $G^\pm$  with  $H^\pm G^\pm A_1$  coupling (in the Feynman gauge) is proportional to  $\tan\beta$ .

For the chargino contributions:

$$C_A^{\chi^C} = i \frac{\tan \beta}{\sqrt{2}} \Gamma_1(i, i, j, l) \left\{ \delta_- \delta_{lj} \frac{v}{s} x_{\chi_j^C}^{1/2} P_1(x_{\tilde{t}_{i-1}} \tilde{\chi}_j^C) \right. \\ \left. - \left[ R_{1jl} x_{\chi_j^C}^{1/2} F_1(x_{\tilde{t}_{i-1}} \tilde{\chi}_l^C, x_{\tilde{\chi}_j^C} \tilde{\chi}_l^C) - R_{1lj}^* F_2(x_{\tilde{t}_{i-1}} \tilde{\chi}_l^C, x_{\tilde{\chi}_j^C} \tilde{\chi}_l^C) \right] \right\}, \quad (\text{A4})$$

$$C_{Q_1}^{\tilde{\chi}^\pm} = \frac{m_b m_l}{4m_{H_a}^2} \tan^2 \beta \sum_{i,k=1}^3 \sum_{j,l=1}^2 \Gamma_1(i, k, j, l) \left\{ \frac{\sqrt{2} U_{a1}^H U_{a1}^H m_{\chi_j^C}}{m_W \cos \beta} \delta_{ik} \delta_{lj} P_1(x_{\tilde{t}_{i-1}} \tilde{\chi}_j^C) \right. \\ \left. - \frac{2\sqrt{2} U_{a1}^H}{g_2} \delta_{ik} \left[ Q_{alj}^* F_2(x_{\tilde{t}_{i-1}} \tilde{\chi}_l^C, x_{\tilde{\chi}_j^C} \tilde{\chi}_l^C) + \frac{m_{\chi_j^C}}{m_{\chi_l^C}} Q_{ajl} F_1(x_{\tilde{t}_{i-1}} \tilde{\chi}_l^C, x_{\tilde{\chi}_j^C} \tilde{\chi}_l^C) \right] \right. \\ \left. + \frac{2\sqrt{2} U_{a1}^H T_2^{aik} m_{\chi_j^C}}{m_{\tilde{t}_{k-1}}^2} \delta_{lj} F_1(x_{\tilde{t}_{i-1}} \tilde{t}_{k-1}, x_{\tilde{\chi}_j^C} \tilde{t}_{k-1}) \right. \\ \left. + \frac{m_{H_a}^2}{m_{\chi_j^C}^2} \delta_{ik} \left[ Z_-^{2j} Z_+^{1l} F_4(x_{\tilde{t}_{i-1}} \tilde{\chi}_j^C, x_{\tilde{\chi}_l^C} \tilde{\chi}_j^C, x_{\tilde{\nu}} \tilde{\chi}_l^C) \right. \right. \\ \left. \left. - \frac{m_{\chi_l^C}}{m_{\chi_j^C}} Z_-^{2l*} Z_+^{1j*} F_3(x_{\tilde{t}_{i-1}} \tilde{\chi}_j^C, x_{\tilde{\chi}_l^C} \tilde{\chi}_j^C, x_{\tilde{\nu}} \tilde{\chi}_l^C) \right] \right\}, \quad (\text{A5})$$

$$C_{Q_2}^{\tilde{\chi}^\pm} = -\frac{m_b m_l}{4m_{A_\alpha}^2} \tan^2 \beta \sum_{i,k=1}^3 \sum_{j,l=1}^2 \Gamma_1(i, k, j, l) \left\{ \frac{\sqrt{2} U_{a1}^A U_{a1}^A m_{\chi_j^C}}{m_W \cos \beta} \delta_{ik} \delta_{lj} P_1(x_{\tilde{t}_{i-1}} \tilde{\chi}_j^C) \right. \\ \left. - \frac{2\sqrt{2} U_{a1}^A}{g_2} \delta_{ik} \left[ -R_{alj}^* F_2(x_{\tilde{t}_{i-1}} \tilde{\chi}_l^C, x_{\tilde{\chi}_j^C} \tilde{\chi}_l^C) + \frac{m_{\chi_j^C}}{m_{\chi_l^C}} R_{ajl} F_1(x_{\tilde{t}_{i-1}} \tilde{\chi}_l^C, x_{\tilde{\chi}_j^C} \tilde{\chi}_l^C) \right] \right. \\ \left. - \frac{\sqrt{2} U_{a1}^A T_1^{\alpha ik} m_t m_{\chi_j^C}}{m_W m_{\tilde{t}_{k-1}}^2} \delta_{lj} F_1(x_{\tilde{t}_{i-1}} \tilde{t}_{k-1}, x_{\tilde{\chi}_j^C} \tilde{t}_{k-1}) \right. \\ \left. + \frac{m_{A_\alpha}^2}{m_{\chi_j^C}^2} \delta_{ik} \left[ Z_-^{2j} Z_+^{1l} F_4(x_{\tilde{t}_{i-1}} \tilde{\chi}_j^C, x_{\tilde{\chi}_l^C} \tilde{\chi}_j^C, x_{\tilde{\nu}} \tilde{\chi}_l^C) \right. \right. \\ \left. \left. - \frac{m_{\chi_l^C}}{m_{\chi_j^C}} Z_-^{2l*} Z_+^{1j*} F_3(x_{\tilde{t}_{i-1}} \tilde{\chi}_j^C, x_{\tilde{\chi}_l^C} \tilde{\chi}_j^C, x_{\tilde{\nu}} \tilde{\chi}_l^C) \right] \right\} \quad (\text{A6})$$

Note that here  $C_{Q_{1,2}}$  contain terms which can be enhanced by  $\tan^3 \beta$  (the overall factor  $\tan^2 \beta$  multiplied by  $1/\cos \beta$  gives  $\tan^3 \beta$  in large  $\tan \beta$  limit).

For neutralino contributions:

$$C_A^{\chi^0} = -\frac{i}{V_{tb} V_{ts}^*} \frac{\tan \beta}{\cos \theta_W} N_j' \left\{ Z_N^{3k*} T_D^{i2} T_D^{i1*} \left[ R_{1jk}'' T_D^{i2} x_{\chi_k^0}^{1/2} F_1(x_{\tilde{b}_{i-1}} \tilde{\chi}_j^0, x_{\tilde{\chi}_k^0} \tilde{\chi}_j^0) \right. \right. \\ \left. \left. - R_{1jk}^{R*''} F_2(x_{\tilde{b}_{i-1}} \tilde{\chi}_j^0, x_{\tilde{\chi}_k^0} \tilde{\chi}_j^0) \right] + T_3^{1ik'} \Gamma_2(i, j, k') (x_{\chi_j^0 \tilde{b}_{k'-1}} x_{W \tilde{b}_{k'-1}})^{1/2} \right. \\ \left. \times F_1(x_{\tilde{b}_{i-1} \tilde{b}_{k'-1}}, x_{\chi_j^0 \tilde{b}_{k'-1}}) + \delta_{ik'} \frac{\delta_- \cot \beta}{\sqrt{2}} \frac{v}{s} x_{\chi_j^0 b}^{1/2} \Gamma_2(i, j, k') P_1(x_{\tilde{b}_{i-1}} \tilde{\chi}_j^0) \right\} \quad (\text{A7})$$



$$\begin{aligned}
C_{Q_1}^{\tilde{\chi}^0} = & -\frac{1}{K_{tb}K_{ts}^*} \frac{m_b m_l}{4m_{H_a}^2 \cos \theta_w} \tan^2 \beta \sum_{i,k'=1}^3 \sum_{j,k=1}^5 \sum_{m=1}^6 N'_j \left\{ \frac{\sqrt{2}U_{a1}^H U_{a1}^H m_{\chi_j^0}}{m_b} \delta_{ik'} \Gamma_2(i, j, k') P_1(x_{\tilde{b}_{i-1}\tilde{\chi}_j^0}) \right. \\
& - \frac{2U_{a1}^H Z_N^{3k*}}{g_2} \left[ Q_{ajk}^{L''} T_D^{i2} T_D^{i1*} F_2(x_{\tilde{b}_{i-1}\tilde{\chi}_j^0}, x_{\tilde{\chi}_k^0 \tilde{\chi}_j^0}) \right. \\
& \left. \left. + Q_{ajk}^{R''} \left( \frac{m_{\chi_k^0}}{m_{\chi_j^0}} T_D^{i2} T_D^{i1*} + \frac{m_b}{m_{\chi_j^0}} T_D^{i3} T_D^{i1*} \right) F_1(x_{\tilde{b}_{i-1}\tilde{\chi}_j^0}, x_{\tilde{\chi}_k^0 \tilde{\chi}_j^0}) \right] \right. \\
& + 2U_{a1}^H \frac{m_{\chi_j^0}}{m_{\tilde{b}_{k'-1}}^2} \left( \frac{1}{\sqrt{2}} T_4^{\alpha ik'} \Gamma_2(i, j, k') + T_5^{\alpha ik'} Z_N^{3j*} T_D^{i1*} T_D^{k'2} \right) F_1(x_{\tilde{b}_{i-1}\tilde{b}_{k'-1}}, x_{\chi_j^0 \tilde{b}_{k'-1}}) \\
& + \frac{m_{H_a}^2}{m_{\chi_k^0}^2} \left[ \left( \frac{m_{\chi_j^0}}{m_{\chi_k^0}} \Gamma_6(i, k) Z_L^{(I+3)m*} Z_L^I Z_N^{3k*} Z_N^{3j*} - \Gamma_7(i, k, j) \right) F_3(x_{\tilde{b}_{i-1}\tilde{\chi}_j^0}, x_{\tilde{\chi}_k^0 \tilde{\chi}_j^0}, x_{\tilde{l}_m \tilde{\chi}_j^0}) \right. \\
& \left. \left. - \left( \Gamma_6(i, k) Z_L^{(I+3)m} Z_L^{Im*} Z_N^{3k} Z_N^{3j} - \Gamma_7(i, j, k) \right) F_4(x_{\tilde{b}_{i-1}\tilde{\chi}_j^0}, x_{\tilde{\chi}_k^0 \tilde{\chi}_j^0}, x_{\tilde{l}_m \tilde{\chi}_j^0}) \right] \right\}, \quad (A8)
\end{aligned}$$

$$\begin{aligned}
C_{Q_2}^{\tilde{\chi}^0} = & \frac{1}{K_{tb}K_{ts}^*} \frac{m_b m_l}{4m_{A_\alpha}^2 \cos \theta_w} \tan^2 \beta \sum_{i,k'=1}^3 \sum_{j,k=1}^5 \sum_{m=1}^6 N'_j \left\{ \frac{\sqrt{2}U_{\alpha 1}^A U_{\alpha 1}^A m_{\chi_j^0}}{m_b} \delta_{ik'} \Gamma_2(i, j, k') P_1(x_{\tilde{b}_{i-1}\tilde{\chi}_j^0}) \right. \\
& + \frac{2U_{\alpha 1}^A Z_N^{3k*}}{g_2} \left[ R_{\alpha jk}^{L''} T_D^{i2} T_D^{i1*} F_2(x_{\tilde{b}_{i-1}\tilde{\chi}_j^0}, x_{\tilde{\chi}_k^0 \tilde{\chi}_j^0}) \right. \\
& \left. + R_{\alpha jk}^{R''} \left( \frac{m_{\chi_k^0}}{m_{\chi_j^0}} T_D^{i2} T_D^{i1*} + \frac{m_b}{m_{\chi_j^0}} T_D^{i3} T_D^{i1*} \right) F_1(x_{\tilde{b}_{i-1}\tilde{\chi}_j^0}, x_{\tilde{\chi}_k^0 \tilde{\chi}_j^0}) \right] \\
& + 2U_{\alpha 1}^A \frac{m_{\chi_j^0}}{m_{\tilde{b}_{k'-1}}^2} T_3^{\alpha ik'} \Gamma_2(i, j, k') F_1(x_{\tilde{b}_{i-1}\tilde{b}_{k'-1}}, x_{\chi_j^0 \tilde{b}_{k'-1}}) \\
& - \frac{m_{A_\alpha}^2}{m_{\chi_k^0}^2} \left[ \left( \frac{m_{\chi_j^0}}{m_{\chi_k^0}} \Gamma_6(i, k) Z_L^{(I+3)m*} Z_L^I Z_N^{3k*} Z_N^{3j*} - \Gamma_7(i, k, j) \right) F_3(x_{\tilde{b}_{i-1}\tilde{\chi}_j^0}, x_{\tilde{\chi}_k^0 \tilde{\chi}_j^0}, x_{\tilde{l}_m \tilde{\chi}_j^0}) \right. \\
& \left. \left. - \left( \Gamma_6(i, k) Z_L^{(I+3)m} Z_L^{Im*} Z_N^{3k} Z_N^{3j} - \Gamma_7(i, j, k) \right) F_4(x_{\tilde{b}_{i-1}\tilde{\chi}_j^0}, x_{\tilde{\chi}_k^0 \tilde{\chi}_j^0}, x_{\tilde{l}_m \tilde{\chi}_j^0}) \right] \right\} \quad (A9)
\end{aligned}$$

For gluino contributions:

$$\begin{aligned}
C_A^{\tilde{g}} = & \frac{i}{V_{tb}V_{ts}^*} \frac{8g_3^2}{3g_2^2} \tan \beta T_D^{j1*} \left[ \delta_{ij} \frac{v}{s} \frac{\delta_-}{\tan \beta} x_{\tilde{g}b}^{1/2} P_1(x_{\tilde{b}_{i-1}\tilde{g}}) \right. \\
& \left. + T_3^{1ji} (x_{\tilde{g}\tilde{b}_{j-1}} x_{W\tilde{b}_{j-1}})^{1/2} F_1(x_{\tilde{b}_{i-1}\tilde{b}_{j-1}}, x_{\tilde{g}\tilde{b}_{j-1}}) \right], \quad (A10)
\end{aligned}$$

$$\begin{aligned}
C_{Q_1}^{\tilde{g}} = & \frac{1}{K_{tb}K_{ts}^*} \frac{m_b m_l}{4} \frac{16g_3^2 m_{\tilde{g}}}{3g_2^2 m_{H_a}^2} \tan^2 \beta \sum_{i,j=1}^3 T_D^{i3} T_D^{j1*} \left[ \frac{U_{a1}^H U_{a1}^H}{m_b} \delta_{ij} P_1(x_{\tilde{b}_{i-1}\tilde{g}}) \right. \\
& \left. + \frac{U_{a1}^H T_4^{\alpha ji}}{m_{\tilde{b}_{j-1}}^2} F_1(x_{\tilde{b}_{i-1}\tilde{b}_{j-1}}, x_{\tilde{g}\tilde{b}_{j-1}}) \right], \quad (A11)
\end{aligned}$$

$$\begin{aligned}
C_{Q_2}^{\tilde{g}} = & -\frac{1}{K_{tb}K_{ts}^*} \frac{m_b m_l}{4} \frac{16g_3^2 m_{\tilde{g}}}{3g_2^2 m_{A_\alpha}^2} \tan^2 \beta \sum_{i,j=1}^3 T_D^{i3} T_D^{j1*} \left[ \frac{U_{\alpha 1}^A U_{\alpha 1}^A}{m_b} \delta_{ij} P_1(x_{\tilde{b}_{i-1}\tilde{g}}) \right. \\
& \left. + \frac{U_{\alpha 1}^A T_3^{\alpha ji}}{m_{\tilde{b}_{j-1}}^2} F_1(x_{\tilde{b}_{i-1}\tilde{b}_{j-1}}, x_{\tilde{g}\tilde{b}_{j-1}}) \right]. \quad (A12)
\end{aligned}$$

In the above expressions the constants and functions are defined by

$$N'_j = \frac{1}{3}Z_N^{1j*} \sin \theta_w - Z_N^{2j*} \cos \theta_w, \quad N''_j = -Z_N^{1j} \sin \theta_w + Z_N^{2j} \cos \theta_w \quad (\text{A13})$$

$$R_{\alpha lj} = -\frac{g_2}{\sqrt{2}}(U_{\alpha 1}^A Z_-^{2l} Z_+^{1j} + U_{\alpha 2}^A Z_-^{1l} Z_+^{2j}) - \frac{\lambda}{\sqrt{2}}U_{\alpha 3}^A Z_-^{2l} Z_+^{2j} \quad (\text{A14})$$

$$Q_{\alpha lj} = \frac{g_2}{\sqrt{2}}(U_{\alpha 1}^H Z_-^{2l} Z_+^{1j} + U_{\alpha 2}^H Z_-^{1l} Z_+^{2j}) - \frac{\lambda}{\sqrt{2}}U_{\alpha 3}^H Z_-^{2l} Z_+^{2j} \quad (\text{A15})$$

$$\begin{aligned} R_{\alpha jk}^{L''} = -R_{\alpha jk}^{R''*} = & -\frac{1}{2}\{-U_{\alpha 2}^A[\frac{g_2}{\cos \theta_w}(Z_N^{4k} N''_j + Z_N^{4j} N''_k) + \sqrt{2}\lambda(Z_N^{5j} Z_N^{3k} + Z_N^{3j} Z_N^{5k})] \\ & + U_{\alpha 1}^A[\frac{g_2}{\cos \theta_w}(Z_N^{3k} N''_j + Z_N^{3j} N''_k) - \sqrt{2}\lambda(Z_N^{5j} Z_N^{4k} + Z_N^{4j} Z_N^{5k})]\} \\ & - \sqrt{2}\kappa U_{\alpha 3}^A(Z_N^{5j} Z_N^{5k} + Z_N^{5j} Z_N^{5k}) \end{aligned} \quad (\text{A16})$$

$$\begin{aligned} Q_{\alpha jk}^{L''} = Q_{\alpha jk}^{R''*} = & \frac{1}{2}\{U_{\alpha 2}^H[\frac{-g_2}{\cos \theta_w}(Z_N^{4k} N''_j + Z_N^{4j} N''_k) + \sqrt{2}\lambda(Z_N^{5j} Z_N^{3k} + Z_N^{3j} Z_N^{5k})] \\ & + U_{\alpha 1}^H[\frac{g_2}{\cos \theta_w}(Z_N^{3k} N''_j + Z_N^{3j} N''_k) + \sqrt{2}\lambda(Z_N^{5j} Z_N^{4k} + Z_N^{4j} Z_N^{5k})]\} \\ & - \sqrt{2}\kappa U_{\alpha 3}^H(Z_N^{5j} Z_N^{5k} + Z_N^{5j} Z_N^{5k}) \end{aligned} \quad (\text{A17})$$

$$\Gamma_1(i, k, j, l) = (T_U^{i2} T_U^{k2*} - \delta_{i1} \delta_{k1}) Z_+^{1l*} Z_-^{2j*} - \frac{m_t}{\sqrt{2}m_W \sin \beta} T_U^{i3} T_U^{k2*} Z_+^{2l*} Z_-^{2j*} \quad (\text{A18})$$

$$\Gamma_2(i, j, k') = \sqrt{2} \tan \theta_w Z_N^{1j*} T_D^{i1*} T_D^{k'3} + \frac{m_b}{\sqrt{2}m_W \cos \beta} Z_N^{3j*} T_D^{i1*} T_D^{k'2} \quad (\text{A19})$$

$$\Gamma_6(i, j) = \frac{m_l \sin \theta_w}{3m_b \cos \theta_w} Z_N^{1j*} T_D^{i1*} T_D^{i3} \quad (\text{A20})$$

$$\begin{aligned} \Gamma_7(i, j, k) = & \frac{1}{2 \cos \theta_w} Z_N^{3j} T_D^{i1*} T_D^{i2} [Z_L^{Im*} Z_L^m (Z_N^{1j*} \sin \theta_w + Z_N^{2j*} \cos \theta_w) Z_N^{3k*} \\ & - 2 \sin \theta_w Z_L^{(I+3)m*} Z_L^{(I+3)m} Z_N^{3j*} Z_N^{1k*}] \end{aligned} \quad (\text{A21})$$

$$T_1^{\alpha ik} = A_3 T_U^{i3*} T_U^{k2} - A_3^* T_U^{i2*} T_U^{k3}, \quad T_3^{\alpha ik} = A_1 T_D^{k2*} T_D^{i3} - A_1^* T_D^{k3*} T_D^{i2} \quad (\text{A22})$$

$$\begin{aligned} T_2^{\alpha ik} = & -\frac{m_t}{2m_W} [2m_t U_{\alpha 2}^H (T_U^{i2*} T_U^{k2} + T_U^{i3*} T_U^{k3}) + (A_4 T_U^{i3*} T_U^{k2} + A_4^* T_U^{i2*} T_U^{k3})] \\ & + A_5 (T_U^{i1*} T_U^{k1} + T_U^{i2*} T_U^{k2}) + A_6 T_U^{i3*} T_U^{k3} \end{aligned} \quad (\text{A23})$$

$$T_4^{\alpha ik} = -2m_t U_{\alpha 1}^H (T_D^{i2} T_D^{k2*} + T_D^{i3} T_D^{k3*}) + (A_2 T_D^{i3} T_U^{k2*} + A_2^* T_U^{i2} T_D^{k3*}) \quad (\text{A24})$$

$$T_5^{\alpha ik} = A_7 T_D^{i3} T_U^{k3*} - A_8 (T_D^{i2} T_D^{k2*} + T_D^{i1} T_D^{k1*}) \quad (\text{A25})$$

$$A_1 = \frac{\lambda}{\sqrt{2}}(v_u U_{\alpha 3}^A + s U_{\alpha 2}^A) - A_D U_{\alpha 1}^A, \quad A_2 = \frac{\lambda}{\sqrt{2}}(v_u U_{\alpha 3}^H + s U_{\alpha 2}^H) + A_D U_{\alpha 1}^H \quad (\text{A26})$$

$$A_3 = \frac{\lambda}{\sqrt{2}}(v_d U_{\alpha 3}^A + s U_{\alpha 1}^A) - A_U U_{\alpha 2}^A, \quad A_4 = \frac{\lambda}{\sqrt{2}}(v_d U_{\alpha 3}^H + s U_{\alpha 1}^H) + A_U U_{\alpha 2}^H \quad (\text{A27})$$

$$A_5 = \frac{m_z}{2 \cos \theta_w} (1 - \frac{4}{3} \sin^2 \theta_w) U_{\alpha 2}^H, \quad A_6 = \frac{2}{3} m_W \tan^2 \theta_w U_{\alpha 2}^H \quad (\text{A28})$$

$$A_7 = m_W e_d \tan^2 \theta_w U_{\alpha 2}^H, \quad A_8 = \frac{m_z}{2 \cos \theta_w} (1 + 2e_d \sin \theta_w) U_{\alpha 2}^H \quad (\text{A29})$$

$$P_1(x) = \frac{x \ln x}{x-1}, \quad F_1(x, y) = \frac{1}{x-y} \left( \frac{x \ln x}{x-1} - \frac{y \ln y}{y-1} \right), \quad (\text{A30})$$

$$F_2(x, y) = \frac{1}{x-y} \left( \frac{x^2 \ln x}{x-1} - \frac{y^2 \ln y}{y-1} \right) \quad (\text{A31})$$

$$F_3(x, y, z) = \frac{x \ln x}{(x-1)(x-y)(x-z)} + \frac{18}{\alpha^2 \ln x} (x \leftrightarrow y) + (x \leftrightarrow z), \quad (\text{A32})$$

- 
- [1] For recent reviews, see, V. Barger, P. Langacker, H.-S. Lee, G. Shaughnessy, Phys. Rev. D **73**,(2006) 115010. V. Barger, P. Langacker, G. Shaughnessy, hep-ph/0611112.
- [2] R. Dermisek, J. F. Gunion, Phys. Rev. Lett. **95**,(2005) 041801; Phys. Rev. D **73**,(2006) 111701.
- [3] X.-G. He, J. Tandean, G. Valencia, Phys. Rev. Lett. **98**, (2007) 081802; Phys. Rev. D **74**, (2006) 115015.
- [4] G. Hiller, Phys. Rev. D **70**,(2004) 034018.
- [5] F. Domingo and U. Ellwanger, arXiv: 0710.3714. For similar studies in the MSSM, see, M. Carena, *et al.*, Phys. Rev. D **74**, 015009 (2006); Phys. Rev. D **76**, 035004 (2007); G. Isidori and P. Paradisi, Phys. Lett. B **639**, 499 (2006); J. Ellis, *et al.*, arXiv: 0706.0652 [hep-ph]; M. Blanke, *et al.*, JHEP 0610, 003 (2006); P. Ball and R. Fleischer, Eur. Phys. J. C **48**, 413 (2006); M. Blanke and A. J. Buras, JHEP 0705, 061 (2007); A. Freitas, E. Gasser and U. Haisch, Phys. Rev. D **76**, 014016 (2007); G. Isidori, *et al.*, Phys. Rev. D **75**, 115019 (2007); W. Altmannshofer, A. J. Buras and D. Guadagnoli, hep-ph/0703200.
- [6] For a review, see, T. Hurth, Rev. Mod. Phys. **75**, 1159 (2003).
- [7] A. Ghinculov, T. Turth, G. Isidori and Y.-P. Yao, Nucl. Phys. B **685**, 351 (2004); F. M. Borzumati and C. Greub, Phys. Rev. D **58**, 074004 (1998); K. Chetykin, M. Misiak, and M. Münz, Phys. Lett. B **400**, 206 (1997); C. Greub and T. Hurth, Phys. Rev. D **56**, 2934 (1997); J. L. Hewett, Phys. Rev. D **53**, 4964 (1996); M. Misiak, Nucl. Phys. B **393**, 23 (1993);
- [8] Y. B. Dai, C. S. Huang and H. W. Huang, Phys. Lett. B **390**, 257 (1997);
- [9] C. S. Huang, W. Liao, Q. Yan, Phys. Rev. D **59**, 011701 (1999); C. S. Huang, S. H. Zhu, Phys. Rev. D **61**, 015011 (2000); C. S. Huang, W. Liao, Q. Yan, S. H. Zhu, Phys. Rev. D **63**, 114021 (2001); Eur. Phys. J. C **25**, 103 (2002); S. R. Choudury, N. Gaur, Phys. Lett. B **451**, 86 (1999).
- [10] T. Goto, Y. Okada, Y. Shinizu and M. Tanada, Phys. Rev. D **55**, 4273 (1997); T. M. Aliev, A. Özpıneci and M. Savci, Phys. Rev. D **55**, 7059 (1997); T. M. Aliev, N. K. Pak and M. Savci, Phys. Lett. B **424**, 175 (1998).
- [11] E. O. Iltan and G. Turan, Phys. Rev. D **61**, 034010 (2000).
- [12] Z. Xiong and J. M. Yang, Nucl. Phys. B **602**, 289 (2001);
- [13] C. Bobeth, T. Ewerth, F. Kruger, J. Urban, Phys. Rev. D **66**, 074021 (2002); G. Erkol, G.

- Turan, JHEP 0202, 015 (2002); Nucl. Phys. B **635**, 286 (2002); S. R. Choudhury, N. Gaur, Phys. Rev. D **66**, 094015 (2002); J. K. Mizukoshi, X. Tata, Y. Wang, Phys. Rev. D **66**, 115003 (2002); Y. B. Dai, C. S. Huang, J. T. Li, W. J. Li, Phys. Rev. D **67**, 096007 (2003); C. S. Huang, X. H. Wu, Nucl. Phys. B **657**, 304 (2003); Y. Wang, D. Atwood, Phys. Rev. D **68**, 094016 (2003); A. S. Cornell, N. Gaur, JHEP 0309, 030 (2003); U. O. Yilmaz, B. B. Sirvanli, G. Turan, Eur. Phys. J. C **30**, 197 (2003); T. Feldmann, J. Matias, JHEP 0301, 074 (2003); T. Ibrahim, P. Nath, Phys. Rev. D **67**, 016005 (2003); P.H. Chankowski, L. Slawianowska, Eur. Phys. J. C **33**, 123 (2004); S. R. Choudhury, A. S. Cornell, N. Gaur, G. C. Joshi, Phys. Rev. D **69**, 054018 (2004); T. M. Aliev, V. Bashiry, M. Savci, JHEP 0405, 037 (2004); Phys. Rev. D **73**, 034013 (2006); H. Acar, G. Turan, Acta Phys. Polon. B35, 687 (2004) [hep-ph/0410125]; U. O. Yilmaz, B. B. Sirvanli, G. Turan, Nucl. Phys. B **692**, 249 (2004); T.-F. Feng, X.-Q. Li, J. Maalampi, Phys. Rev. D **73**, 035011 (2006); Z. Xiong and J. M. Yang, Nucl. Phys. B **628**, 193 (2002); Y. Su, Phys. Rev. D **56**, 335 (1997).
- [14] D. J. Miller, R. Nevzorov and P. M. Zerwas, Nucl. Phys. B **681**, 3 (2004);
- [15] K. I. Hikasa and M. Kobayashi, Phys. Rev. D **36**, 724 (1987).
- [16] U. Ellwanger, J. F. Gunion, C. Hugonie, JHEP **0502**:066(2005).
- [17] E. Lunghi, A. Masiero, I. Scimemi, L. Silvestrini, Nucl. Phys. B **568**, 120 (2000).
- [18] S. Bertolini, F. Borzumati, A. Masiero and G. Ridolfi, Nucl. Phys. B **353**, 591 (1991); A. J. Buras and M. Münz, Phys. Rev. D **52**, 186 (1995); P. Cho, M. Misiak and D. Wyler, Phys. Rev. D **54**, (1996) 3329; M. Ciuchini, G. Degrossi, P. Gambino and G. F. Giudice, Nucl. Phys. B **527**, 21 (1998); Nucl. Phys. B **534**,3 (1998).
- [19] J.Kaneko, *et al.*, Phys. Rev. Lett. **90**, 021801 (2003).
- [20] E. Barberio, *et al.*, Heavy Flavor Averaging Group (HFAG), hep-ex/0603003 (webpage: [www.slac.stanford.edu/xorg/hfag](http://www.slac.stanford.edu/xorg/hfag)).
- [21] W.M. Yao *et al.*, J. Phys. G **33**, 1 (2006).
- [22] A. Ali, G. Hiller, L. T. Handoko and T. Morozumi, Phys. Rev. D **55**, 4105 (1997).
- [23] Z. Xiong and J. M. Yang, Phys. Lett. B **546**, (2002) 221